



**Source areas and trajectories of nucleating air masses**

Z. Németh and I. Salma

# Source areas and trajectories of nucleating air masses within and near the Carpathian Basin

**Z. Németh and I. Salma**

Institute of Chemistry, Eötvös University, Budapest, Hungary

Received: 19 February 2014 – Accepted: 24 March 2014 – Published: 4 April 2014

Correspondence to: I. Salma (salma@chem.elte.hu)

Published by Copernicus Publications on behalf of the European Geosciences Union.

Title Page

Abstract

Introduction

Conclusions

References

Tables

Figures

◀

▶

◀

▶

Back

Close

Full Screen / Esc

Printer-friendly Version

Interactive Discussion

## Abstract

Particle number size distributions were measured by differential mobility particle sizer in the diameter range of 6–1000 nm in the near-city background and city centre of Budapest continuously for two years. The city is situated in the middle part of the Carpathian Basin, which is a topographically discrete unit in the southeast Central Europe. Yearly mean nucleation frequencies and uncertainties for the near-city background and city centre were  $(28 \pm 6 / -4) \%$  and  $(27 \pm 9 / -4) \%$ , respectively. Total numbers of days with continuous and uninterrupted growth process were 43 and 31, respectively. These events and their properties were utilised to investigate if there are any specific tracks and/or separable source regions for the nucleating air masses within or near the basin. Local wind speed and direction data indicated that there seem to be differences between the nucleation and growth intervals and non-nucleation days. For further analysis, backward trajectories were generated by a simple air parcel trajectory model. Start and end time parameters of the nucleation, and end time parameter of the particle growth were derived by a standardized procedure based on examining the channel contents of the contour plots. These parameters were used to specify a segment on each air mass trajectory that is associated with the track of the nucleating air mass. The results indicated that the nucleation events happened in the continental boundary layer mostly within the Carpathian Basin but the most distant trajectories originated outside of the basin. The tracks of the nucleating air masses were predominantly associated with NW and SE geographical fields, while the source areas that could be separated were frequently situated in the NW and NE quarters. Many of them were within or close to large forested territories. The results also emphasize that the new particle formation and growth phenomenon that occurs in the region influences larger territories than the Carpathian Basin.

ACPD

14, 9225–9247, 2014

### Source areas and trajectories of nucleating air masses

Z. Németh and I. Salma

Title Page

Abstract

Introduction

Conclusions

References

Tables

Figures

◀

▶

◀

▶

Back

Close

Full Screen / Esc

Printer-friendly Version

Interactive Discussion

# 1 Introduction

It is increasingly recognised that ultrafine (UF) aerosol particles influence our life and environment in many important ways. One of their sources is atmospheric nucleation. Field measurements suggest that nucleation is a worldwide phenomenon (Kulmala et al., 2004), and that nucleation is a substantial source of these particles (Spracklen et al., 2010; Yu et al., 2010). In addition, the freshly nucleated particles are able to grow into size ranges where they can act as cloud condensation nuclei (CCN) (Laaksonen et al., 1998; Andreae and Rosenfeld, 2008; Wiedensohler et al., 2009), which are associated with important indirect radiative effects in the climate system (Wang and Penner, 2009; Kerminen et al., 2012; Makkonen et al., 2012). Global model investigations indicate that at least 50 % of CCN is formed by condensational growth of nucleated particles (Merikanto et al., 2009). Even in urban environments, contribution of nucleation to UF particle concentrations with respect to all sources is between 23 % and 43 % in spring and summer (Salma et al., 2013). This emphasizes the possibility of significant health consequences of nucleated particles in cities – in addition to their climate relevance. Ultrafine aerosol represents excess health risk relative to coarse or fine particles of similar chemical composition (Oberdörster et al., 2005) due to the large number of insoluble particles that can be deposited in the upper respiratory system (mainly nose), their large surface area and very small size (Kreyling et al., 2006; HEI Review Panel, 2013).

New particle formation and particle growth events were identified on the regional scale in a variety of geographic locations around the world (Kulmala et al., 2004; Kulmala and Kerminen, 2008). In clean environments, horizontal extension of the nucleating air masses can reach up to hundreds of kilometers (Kulmala et al., 1998, 2001; Vana et al., 2004; Komppula et al., 2006; Väänänen et al., 2013). As far as the vertical occurrence is concerned, nucleation was observed at altitudes ranging from surface locations (Kulmala et al., 2004) up to the free and upper troposphere (Clarke et al., 1998, 1999; Minikin et al., 2003). In addition, several long-term observations indicated

ACPD

14, 9225–9247, 2014

## Source areas and trajectories of nucleating air masses

Z. Németh and I. Salma

Title Page

Abstract

Introduction

Conclusions

References

Tables

Figures

◀

▶

◀

▶

Back

Close

Full Screen / Esc

Printer-friendly Version

Interactive Discussion

## Source areas and trajectories of nucleating air masses

Z. Németh and I. Salma

Title Page

Abstract

Introduction

Conclusions

References

Tables

Figures

◀

▶

◀

▶

Back

Close

Full Screen / Esc

Printer-friendly Version

Interactive Discussion

that there can be some source regions for nucleating air masses (Coe et al., 2000; Fiedler et al., 2005; Hussein et al., 2009; Komppula et al., 2006; Young et al., 2007). For instance, Kristensson et al. (2008) suggested that there is a relationship between the new particle formation and ship emissions; Hirsikko et al. (2013) reported a source area which was nearby their measurement site in a savannah, and nucleation events observed at SMEAR-2 station in Hyytiälä (Finland) were linked to air masses which frequently originated from the Baltic Sea (Kristensson et al., 2013).

The Carpathian Basin is a topographically discrete unit situated in the southeast Central Europe. Its central part (mainly lowlands) is surrounded by the Alps from the West, by the Carpathian Mountains from the North and East, and by the Dinaric Alps and Balkan Mountains from the South, which represent important barriers to the movements of air masses. Linear dimensions of the basin in the N–S and W–E directions are approximately 300 and 500 km, respectively. These extensions are comparable to distances into which nucleating air masses can ordinarily reach. There are some extensive wooded areas within the Carpathian Basin (in the surrounding mountains and Transylvania) with expectedly cleaner regional air, which can be, however, loaded by biogenic precursor gases. There is a two-year long new particle formation and growth event data set available for Budapest, which is situated in the middle part of the basin. Concentration and other physical properties of the nucleated and UF particles in Budapest were characterised earlier (Salma et al., 2011, 2013). It is just noted here that yearly median particle number concentrations in the near-city background and city centre of Budapest were  $3.4 \times 10^3 \text{ cm}^{-3}$  and  $11.8 \times 10^3 \text{ cm}^{-3}$ , respectively. The major objectives of the present paper are to investigate and discuss if there are preferred directions and source areas for the nucleating air masses in the Carpathian Basin, and to improve the available method for assessing the source regions.

## 2 Methods

### 2.1 Experimental

Particle number size distributions were continuously measured at two sites in Budapest, Hungary for one year each. Between 3 November 2008 and 2 November 2009, the measurements were carried out in the city centre at an open area near the Danube (Lágymányos Campus of the Eötvös University, 47.474° N, 19.062° E, 114 m a.m.s.l.) (Salma et al., 2011). From 19 January 2012 to 18 January 2013, the measurements were realized in a near-city background at the NW border of the city in a wooded area (Konkoly Observatory of the Hungarian Academy of Sciences, 47.500° N, 18.963° E, 478 m a.m.s.l.). The measuring system consisted of an identical flow-switching type differential mobility particle sizer (DMPS) and a meteorological station. The main components of the DMPS system are a  $^{241}\text{Am}$  neutralizer, Nafion semi-permeable membrane dryer, 28 cm long Hauke-type differential mobility analyser (DMA) and a butanol-based condensation particle counter (CPC, model 3775, TSI, USA) (Salma et al., 2011). Particles with an electrical mobility diameter from 6 to 1000 nm are recorded in their dry state in 30 channels. The DMPS measurements were performed according to the recommendations of the international technical standards (Wiedensohler et al., 2012). Basic meteorological data including wind speed (WS) and wind direction (WD) were obtained from the Urban Climatological Station of the Hungarian Meteorological Service operated within the university campus above the rooftop level, or from an on-site meteorological station at a height of 2 m from the ground at the near-city background. Time resolution of all measurements was 10 min.

### 2.2 Data treatment and modelling

The DMPS data were inverted and were represented in contour plots showing the time evolution of normalized particle number concentration and particle diameter on a daily basis. The measurement days were then sorted into evident nucleation events,

unambiguous non-nucleation days, undefined and unclassified days (Dal Maso et al., 2005). In the present study, nucleation events with continuous and uninterrupted growth process, namely class 1A were considered. Wind speed and wind direction data were utilised to create wind roses that are based on the modern Beaufort scale separately for non-nucleation days, and nucleation and growth intervals for class 1A event. For the former case, wind data for the whole day were included. For the event intervals, a narrower time interval that started 1 h before the onset of the nucleation and ended 6 h after the onset of the nucleation (thus from  $t_1 - 1$  h to  $t_1 + 6$  h, see later) was taken into consideration.

Retrospective movement of the nucleating air masses was assessed by backward trajectories generated by the HYSPLIT code version 4.9 (Draxler and Rolph, 2013). The principle of the process was described earlier as NanoMap for remote regions (Kristensson et al., 2013). Three time parameters are required for each nucleation event (banana curve) in order to calculate the set of trajectories and to locate the most distant segment on each trajectory. The time parameters are the following: the end time parameter of the particle growth process ( $t_e$ ), start time parameter ( $t_1$ ) and end time parameter ( $t_2$ ) of the nucleation process. Further steps of the treatment are illustrated on a contour plot in Fig. 1. The particles that arrived to the measurement site at time  $t_e$  had been generated previously at a site (line source) expressed by the end segment of the corresponding backward trajectory. The limiting points of the segment are determined by the time points of  $t_e - t_1$  and  $t_e - t_2$ . Similarly, the particles that arrived to the measurement site at time  $t_e - 1$  h had been generated at a location expressed by a trajectory segment that corresponds to the arrival time  $t_e - 1$  h time and limiting parameters of  $t_e - t_1 - 1$  h and  $t_e - t_2 - 1$  h. The trajectories were calculated and their segments were determined consecutively for arrival times that were repeatedly decreased by 1 h, thus for  $t_e$ ,  $t_e - 1$  h,  $t_e - 2$  h, ... until the difference between the  $t_e$  and  $t_2$  became 1 h. The set of the segments marks the track of the nucleating air mass with a time resolution of 1 h. The endpoints of the segments for all consecutive

## Source areas and trajectories of nucleating air masses

Z. Németh and I. Salma

Title Page

Abstract

Introduction

Conclusions

References

Tables

Figures

◀

▶

◀

▶

Back

Close

Full Screen / Esc

Printer-friendly Version

Interactive Discussion

trajectories were finally connected, and the resulted area represents the movement of a particular nucleating air mass.

In cities, the atmospheric environment usually has more complex or dynamic character than in remote regions. Determination of the time parameters was, therefore, more rigorous in our study. The end time parameter ( $t_e$ ) of the growth was set at the point when (1) the particle growth was evidently finished in the contour plot, or (2) the nucleation mode increasing in the diameter joined the Aitken mode, or (3) substantial direct emissions occurred locally (for more than 1 h). Determination of the  $t_1$  and  $t_2$  time parameters was based on the content of the first channel. A relative method was developed to consider the fact that the particle number concentration can vary substantially among different (urban) environments (Salma et al., 2013). First, the maximum of the normalised concentration in the first channel ( $c_{\max}$ ) was localised. For the city centre, the  $t_1$  and  $t_2$  time parameters were set before and after  $c_{\max}$ , respectively at a concentration level of  $c_{\max}/4$  if  $c_{\max} > 40 \times 10^3 \text{ cm}^{-3}$ , they were set at  $c_{\max}/3$  level if  $c_{\max}$  was between  $30 \times 10^3$  and  $40 \times 10^3 \text{ cm}^{-3}$ , and they were assigned to  $c_{\max}/2$  if  $c_{\max} < 30 \times 10^3 \text{ cm}^{-3}$ . For the near-city background, these cut-off concentrations differed due to lower concentration levels and larger relative differences among the channel contents. If  $c_{\max} > 30 \times 10^3 \text{ cm}^{-3}$ , then the time parameters were set at  $c_{\max}/5$ , if  $c_{\max}$  was between  $15 \times 10^3$  and  $30 \times 10^3 \text{ cm}^{-3}$ , then they were assigned to  $c_{\max}/4$ , and if  $c_{\max} < 15 \times 10^3 \text{ cm}^{-3}$ , then they were set at  $c_{\max}/3$ . The proposed schema represents a simple but effective method that handles fluctuating data reasonably well. Finally, the time parameters were shifted to smaller value by a time interval that corresponds to the particle growth from 2 nm to the lower diameter detection limit of the DMPS (here 6 nm) utilizing the actual growth rate value. It was assumed implicitly that the nucleation takes places around 2 nm, which is in line with recent direct observations of atmospheric molecular clusters (Kulmala et al., 2013).

For the actual HYSPLIT modelling, embedded meteorological data from the GDAS database were utilized, and trajectories arriving to the receptor sites at a height of 200, 500, 2300 m a.g.l. were calculated. The first height level has the main importance since

## Source areas and trajectories of nucleating air masses

Z. Németh and I. Salma

Title Page

Abstract

Introduction

Conclusions

References

Tables

Figures

◀

▶

◀

▶

Back

Close

Full Screen / Esc

Printer-friendly Version

Interactive Discussion

the measurements were performed near the surface, and the other two heights were selected for checking and comparative purposes.

### 3 Results

#### 3.1 Nucleation frequencies

Total numbers of evident nucleation days, of obvious non-event days, and of undefined days relative to the number of all relevant days in each month for the near-city background and city centre are shown in Fig. 2a and b, respectively. The number of undefined days was regarded as the largest reasonably possible overestimation (if all events were misclassified as undefined day), while negative misclassification of one event day as non-event day in a month was considered as the maximum sensible extend of underestimation. In this way, yearly mean nucleation frequencies and uncertainties for the near-city background and city centre were  $(28 + 6 / - 4) \%$  and  $(27 + 9 / - 4) \%$ , respectively. The two frequencies are within the uncertainty limits, and are very close to each other. The values are considerably large (cf. Kulmala et al., 2004; Kerminen et al., 2012), and also somewhat larger than for many other urban environments. The nucleation frequency is known to be related to local properties (Kiendler-Scharr et al., 2009). The monthly mean frequencies exhibited a remarkable seasonal variation with a minimum in winter, and two local maxima. In the near-city background, two similar maxima occurred in March and September. In the city centre, the largest frequency happened in April, and a smaller maximum appeared in September. The shift in the spring maxima for the two locations could easily be caused by differences between the particular years, and a longer-term observation has been in progress to refine this feature. There were 43 and 31 nucleation days with continuous and uninterrupted growth process (i.e., class 1A) for the near-city background and city centre, respectively. Detailed nucleation and growth properties are to be presented and discussed in a later article from another research aspect.

### Source areas and trajectories of nucleating air masses

Z. Németh and I. Salma

Title Page

Abstract

Introduction

Conclusions

References

Tables

Figures



Back

Close

Full Screen / Esc

Printer-friendly Version

Interactive Discussion





## 3.2 Local wind speed and direction

Overview statistics on the WS data at the city centre and near-city background for all days, and separately for non-nucleation days, nucleation and growth interval of class 1A events is given in Table 1. The wind speed data in the city centre and near-city background were obtained at rather different altitudes of the meteorological sensors, and, therefore, the two sites are not comparable. In the city centre, there are no significant differences between the corresponding average (median and mean) wind speed values for the event intervals and non-nucleation days, while the average wind speed data for the urban background suggest that new particle formation and growth can be related to somewhat higher wind speeds. Prevailing local wind direction was N and NE (22 % and 20 %, respectively of all data) in the city centre, and SW and S (31 % and 19 %, respectively) in the background. The difference can be explained by the actual location of the measurement sites (wind channel above the Danube at the city centre, and higher altitude of the background site). The wind roses for the non-nucleation days and event intervals in the city centre and near-city background are shown in Fig. 3. It is seen that the dominant local wind direction for the non-nucleation days in the city centre is NE–N. The average wind speeds for the different directions varied from 1.7 (SE) to 4.5 ms<sup>-1</sup> (NW). The nucleation and growth intervals, however, are related to prevailing directions of SE and S. The direction-dependent mean wind speed varied from 2.4 (E) to 4.3 ms<sup>-1</sup> (NW). In the near-city background, the dominant local wind direction was SW–S for the non-nucleation days. The average wind speed for the different directions varied from 0.13 (SE) to 0.32 (N) ms<sup>-1</sup>. The nucleation and growth intervals were unambiguously associated with SW (44 % of all intervals) prevailing local wind directions. The direction-dependent mean wind speed varied from 0.26 (E) to 0.53 (SW) ms<sup>-1</sup>. This collectively implies that there seems to be a preferred wind direction during the nucleation and growth intervals from the southern geographical sectors.

### Source areas and trajectories of nucleating air masses

Z. Németh and I. Salma

Title Page

Abstract

Introduction

Conclusions

References

Tables

Figures

◀

▶

◀

▶

Back

Close

Full Screen / Esc

Printer-friendly Version

Interactive Discussion

### 3.3 Tracks and the origin of nucleating air masses

The tracks of the nucleating air masses derived by the method described in Sect. 2.2 for the city centre and near-city background are shown in maps in Figs. 4 and 5, respectively. One event out of 43 cases in the near-city background was not evaluated because of some unfavourable particle growth properties. The tracks are shown in yellow, and their overlapping sections (with multiplicity) are indicated in dark yellow (1×), orange (2×) and red (3×) colours. It is noted that the overall area of tracks depend sensitively on the actual meteorological parameters, mainly wind speed. The tracks for the near-city background have a more complex character than for the city centre. It can be explained by the higher altitude of the background site (than for the city), for which the more open topographical character causes longer trajectories, longer trajectory segments, and larger areas in general. The map was divided into 4 field sectors (quarters) at the measurement sites considering the overall orientation of the tracks, thus with horizontal and vertical axes. For the city centre, there were 8 and 13 tracks arriving from the NW and the SE quarters, while 5 tracks arrived from NE and SW quarters each. For the background, the NW quarter with 20 tracks was absolutely dominating. There were 6 tracks in the NE, and 8 tracks in the SE and SW quarters each. The tracks indicate that the nucleating air masses preferably arrived from the NW or SE quarters. The direction of NW can be also biased with the regionally prevailing wind direction of NW, while the detailed explanation for the direction of SE needs further studies mainly on longer data sets. The tracks also imply indirectly that the air masses arriving from the city centre to the near-city background may influence the nucleation and growth events and their properties in the surroundings. Further experimental investigations at several sites in parallel are required to prove and quantify these interactions. Figures 4 and 5 also show that there were tracks which originated outside of the Carpathian Basin. For the city centre and near-city background, mean distance from the measurement site and its standard deviation for the longest relevant time parameter ( $t_1$ ) were  $(121 \pm 102)$  km and  $(238 \pm 160)$  km, respectively. The difference between them

#### Source areas and trajectories of nucleating air masses

Z. Németh and I. Salma

Title Page

Abstract

Introduction

Conclusions

References

Tables

Figures

◀

▶

◀

▶

Back

Close

Full Screen / Esc

Printer-friendly Version

Interactive Discussion

## Source areas and trajectories of nucleating air masses

Z. Németh and I. Salma

Title Page

Abstract

Introduction

Conclusions

References

Tables

Figures

◀

▶

◀

▶

Back

Close

Full Screen / Esc

Printer-friendly Version

Interactive Discussion

can be again related to the higher altitude of the background site. For the city centre, mean height and its standard deviation of the starting points (for the time parameter  $t_1$ ) were  $(221 \pm 134)$  m, while the mean mixing layer depth and its standard deviation were  $(1013 \pm 432)$  m. For the near-city background, the mean height and its standard deviation of the starting points were  $(398 \pm 291)$  m, while the mean mixing layer depth and its standard deviation were  $(460 \pm 255)$  m. These all mean that the nucleation events identified in Budapest occurred in the planetary boundary layer, but the nucleating air masses originated both inside and outside the Carpathian Basin.

The most distant relevant point of a track indicates the area where the new particle formation event was likely started. Indirect evidence suggests that the extension of the nucleating air masses observed in Budapest is comparable in most cases to the linear dimensions of the city (Salma et al., 2011). Therefore, the area of the city was projected by the backward trajectories that arrived at the slightly different spatial coordinates within Budapest at time  $t_e$  to the two limiting points of the segment on the longest trajectory (thus to the time intervals of  $t_e - t_1$  and  $t_e - t_2$ ). The source area of the nucleating air mass is expected to be within or near them, and therefore, the projected areas were joined into a polygon. The individual source areas of the nucleating air masses and their cross sectional overlaps are shown in a map in Fig. 6. It is important to note that only those cases were included for which the end of the particle growth process could be clearly identified in the contour plot. The total number of these cases was 32. It is seen in this figure that the source areas are situated in accordance to the tracks, hence they are frequently located in the NW and NE field sectors. More importantly, many of them are within or close to larger forested territories. It is noted at the same time that source areas in rather limited number was observed in the Eastern direction, and in Transylvania, which has considerable forests. Spatial distribution of the nucleating tracks and possible source areas outlined in the present paper can be likely improved or further limited as longer data sets and larger number of nucleation and particle growth events will be available from continuous measurements.

*Acknowledgements.* Financial support by the Hungarian Scientific Research Fund (contract K84091) is appreciated. The authors thank to M. Gede of the Eötvös University, Department of Cartography and Geoinformatics for his assistance in generating the maps, and P. Ábrahám, director, G. Mező and A. Holl, researchers of the Konkoly Observatory of the Hungarian Academy of Sciences for their support during the field measurement there.

## References

- Andreae, M. O. and Rosenfeld, D.: Aerosol–cloud–precipitation interactions, Part 1. The nature and sources of cloud-active aerosols, *Earth-Sci. Rev.*, 89, 13–41, 2008.
- Clarke, A., Davis, D., Kapustin, V., Eisele, F., Chen, G., Paluch, I., Lenschow, D., Bandy, A., Thornton, D., Moore, K., Mauldin, L., Tanner, D., Litchy, M., Carroll, M., Collins, J., and Albercook, G.: Particle nucleation in the tropical boundary layer and its coupling to marine sulfur sources, *Science*, 282, 89–92, 1998.
- Clarke, A., Eisele, F., Kapustin, V., Moore, K., Tanner, D., Mauldin, L., Litchy, M., Lienert, B., Carroll, M., and Albercook, G.: Nucleation in the equatorial free troposphere: favorable environments during PEM-Tropics, *J. Geophys. Res.*, 104, 5735–5744, 1999.
- Coe, H., Williams, P. I., McFiggans, G., Gallagher, M. W., Beswick, K. M., Bower, K. N., and Choularton, T. W.: Behavior of ultrafine particles in continental and marine air masses at a rural site in the UK, *J. Geophys. Res.*, 105, 26891–26905, 2000.
- Dal Maso, M., Kulmala, M., Riipinen, I., Wagner, R., Hussein, T., Aalto, P. P., and Lehtinen, K. E. J.: Formation and growth of fresh atmospheric aerosols: eight years of aerosol size distribution data from SMEAR II, Hyytiälä, Finland, *Boreal Environ. Res.*, 10, 323–336, 2005.
- Draxler, R. R. and Rolph, G. D.: HYSPLIT (HYbrid Single-Particle Lagrangian Integrated Trajectory) Model, available at: <http://www.arl.noaa.gov/HYSPLIT.php> (last access: 20 February 2014), NOAA Air Resources Laboratory, College Park, MD, 2013.
- Fiedler, V., Dal Maso, M., Boy, M., Aufmhoff, H., Hoffmann, J., Schuck, T., Birmili, W., Hanke, M., Uecker, J., Arnold, F., and Kulmala, M.: The contribution of sulphuric acid to atmospheric particle formation and growth: a comparison between boundary layers in Northern and Central Europe, *Atmos. Chem. Phys.*, 5, 1773–1785, doi:10.5194/acp-5-1773-2005, 2005.

## Source areas and trajectories of nucleating air masses

Z. Németh and I. Salma

Title Page

Abstract

Introduction

Conclusions

References

Tables

Figures

◀

▶

◀

▶

Back

Close

Full Screen / Esc

Printer-friendly Version

Interactive Discussion



- HEI Review Panel on Ultrafine Particles: Understanding the Health Effects of Ambient Ultrafine Particles, HEI Perspectives 3, Health Effects Institute, Boston, 2013.
- Hirsikko, A., Vakkari, V., Tiitta, P., Hatakka, J., Kerminen, V.-M., Sundström, A.-M., Beukes, J. P., Manninen, H. E., Kulmala, M., and Laakso, L.: Multiple daytime nucleation events in semi-clean savannah and industrial environments in South Africa: analysis based on observations, *Atmos. Chem. Phys.*, 13, 5523–5532, doi:10.5194/acp-13-5523-2013, 2013.
- Hussein, T., Junninen, H., Tunved, P., Kristensson, A., Dal Maso, M., Riipinen, I., Aalto, P. P., Hansson, H.-C., Swietlicki, E., and Kulmala, M.: Time span and spatial scale of regional new particle formation events over Finland and Southern Sweden, *Atmos. Chem. Phys.*, 9, 4699–4716, doi:10.5194/acp-9-4699-2009, 2009.
- Kerminen, V.-M., Paramonov, M., Anttila, T., Riipinen, I., Fountoukis, C., Korhonen, H., Asmi, E., Laakso, L., Lihavainen, H., Swietlicki, E., Svenningsson, B., Asmi, A., Pandis, S. N., Kulmala, M., and Petäjä, T.: Cloud condensation nuclei production associated with atmospheric nucleation: a synthesis based on existing literature and new results, *Atmos. Chem. Phys.*, 12, 12037–12059, doi:10.5194/acp-12-12037-2012, 2012.
- Kiendler-Scharr, A., Wildt, J., Dal Maso, M., Hohaus, T., Kleist, E., Mentel, T. F., Tillmann, R., Uerlings, R., Schurr, U., and Wahner, A.: New particle formation in forests inhibited by isoprene emissions, *Nature*, 461, 381–384, 2009.
- Komppula, M., Sihto, S.-L., Korhonen, H., Lihavainen, H., Kerminen, V.-M., Kulmala, M., and Viisanen, Y.: New particle formation in air mass transported between two measurement sites in Northern Finland, *Atmos. Chem. Phys.*, 6, 2811–2824, doi:10.5194/acp-6-2811-2006, 2006.
- Kreyling, W. G., Semmler-Behnke, M., and Möller, W.: Ultrafine particle-lung interactions: does size matter?, *J. Aerosol Med.*, 19, 74–83, 2006.
- Kristensson, A., Dal Maso, M., Swietlicki, E., Hussein, T., Zhou, J., Kerminen, V.-M., and Kulmala, M.: Characterization of new particle formation events at a background site in Southern Sweden: relation to air mass history, *Tellus B*, 60, 330–344, 2008.
- Kristensson, A., Johansson, M., Swietlicki, E., Kivekäs, N., Hussein, T., Nieminen, T., Junninen, H., Tunved, P., Kulmala, M., and Dal Maso, M.: NanoMap: geographical mapping of atmospheric new particle formation through analysis of particle number size distribution data, *Boreal Environ. Res.*, submitted, 2013.
- Kulmala, M. and Kerminen, V.-M.: On the formation and growth of atmospheric nanoparticles, *Atmos. Res.*, 90, 132–150, 2008.

## Source areas and trajectories of nucleating air masses

Z. Németh and I. Salma

Title Page

Abstract

Introduction

Conclusions

References

Tables

Figures

◀

▶

◀

▶

Back

Close

Full Screen / Esc

Printer-friendly Version

Interactive Discussion



## Source areas and trajectories of nucleating air masses

Z. Németh and I. Salma

Title Page

Abstract

Introduction

Conclusions

References

Tables

Figures

◀

▶

◀

▶

Back

Close

Full Screen / Esc

Printer-friendly Version

Interactive Discussion

- Kulmala, M., Toivonen, A., Mäkelä, J., and Laaksonen, A.: Analysis of the growth of nucleation mode particles observed in boreal forest, *Tellus B*, 50, 449–462, 1998.
- Kulmala, M., Dal Maso, M., Mäkelä, J., Pirjola, L., Väkevä, M., Aalto, P., Miikkulainen, P., Hämeri, K., and O'Dowd, C.: On the formation, growth and composition of nucleation mode particles, *Tellus B*, 53, 479–490, 2001.
- Kulmala, M., Vehkamäki, H., Petäjä, T., Dal Maso, M., Lauri, A., Kerminen, V., Birmili, W., and McMurry, P.: Formation and growth rates of ultrafine atmospheric particles: a review of observations, *J. Aerosol Sci.*, 35, 143–176, 2004.
- Kulmala, M., Kontkanen, J., Junninen, H., Lehtipalo, K., Manninen, H. E. Nieminen, T., Petäjä, T., Sipilä, M., Schobesberger, S., Rantala, P., Franchin, A., Jokinen, T., Järvinen, E., Äijälä, M., Kangasluoma, J., Hakala, J., Aalto, P. P., Paasonen, P., Mikkilä, J., Vanhanen, J., Aalto, J., Hakola, H., Makkonen, U., Ruuskanen, T., Mauldin III, R. L., Duplissy, J., Vehkamäki, H., Bäck, J., Kortelainen, A., Riipinen, I., Kurtén, T., Johnston, M. V., Smith, J. N., Ehn, M., Mentel, T. F., Lehtinen, K. E. J., Laaksonen, A., Kerminen, V.-M., and Worsnop, D. R.: Direct observations of atmospheric aerosol nucleation, *Science*, 339, 943–946, 2013.
- Laaksonen, A., Korhonen, P., Kulmala, M., and Charlson, R. J.: Modification of the Köhler equation to include soluble trace gases and slightly soluble substances, *J. Atmos. Sci.*, 55, 853–862, 1998.
- Makkonen, R., Asmi, A., Kerminen, V.-M., Boy, M., Arneth, A., Hari, P., and Kulmala, M.: Air pollution control and decreasing new particle formation lead to strong climate warming, *Atmos. Chem. Phys.*, 12, 1515–1524, doi:10.5194/acp-12-1515-2012, 2012.
- Merikanto, J., Spracklen, D. V., Mann, G. W., Pickering, S. J., and Carslaw, K. S.: Impact of nucleation on global CCN, *Atmos. Chem. Phys.*, 9, 8601–8616, doi:10.5194/acp-9-8601-2009, 2009.
- Minikin, A., Petzold, A., Ström, J., Krejci, R., Seifert, M., van Velthoven, P., Schlager, H., and Schumann, U.: Aircraft observations of the upper tropospheric fine particle aerosol in the Northern and Southern Hemispheres at midlatitudes, *Geophys. Res. Lett.*, 30, 1503, doi:10.1029/2002GL016458, 2003.
- Oberdörster, G., Oberdörster, E., and Oberdörster, J.: Nanotoxicology: an emerging discipline evolving from studies of ultrafine particles, *Environ. Health Persp.*, 113, 823–839, 2005.

Salma, I., Borsós, T., Weidinger, T., Aalto, P., Hussein, T., Dal Maso, M., and Kulmala, M.: Production, growth and properties of ultrafine atmospheric aerosol particles in an urban environment, *Atmos. Chem. Phys.*, 11, 1339–1353, doi:10.5194/acp-11-1339-2011, 2011.

Salma, I., Borsós, T., Németh, Z., Weidinger, T., Aalto, P., and Kulmala, M.: Comparative study of ultrafine atmospheric aerosol within a city, *Atmos. Environ.*, submitted, 2013.

Spracklen, D. V., Carslaw, K. S., Merikanto, J., Mann, G. W., Reddington, C. L., Pickering, S., Ogren, J. A., Andrews, E., Baltensperger, U., Weingartner, E., Boy, M., Kulmala, M., Laakso, L., Lihavainen, H., Kivekäs, N., Komppula, M., Mihalopoulos, N., Kouvarakis, G., Jennings, S. G., O'Dowd, C., Birmili, W., Wiedensohler, A., Weller, R., Gras, J., Laj, P., Sellegri, K., Bonn, B., Krejci, R., Laaksonen, A., Hamed, A., Minikin, A., Harrison, R. M., Talbot, R., and Sun, J.: Explaining global surface aerosol number concentrations in terms of primary emissions and particle formation, *Atmos. Chem. Phys.*, 10, 4775–4793, doi:10.5194/acp-10-4775-2010, 2010.

Väänänen, R., Kyrö, E.-M., Nieminen, T., Kivekäs, N., Junninen, H., Virkkula, A., Dal Maso, M., Lihavainen, H., Viisanen, Y., Svenningsson, B., Holst, T., Arneth, A., Aalto, P. P., Kulmala, M., and Kerminen, V.-M.: Analysis of particle size distribution changes between three measurement sites in northern Scandinavia, *Atmos. Chem. Phys.*, 13, 11887–11903, doi:10.5194/acp-13-11887-2013, 2013.

Vana, M., Kulmala, M., Dal Maso, D., Hörrak, M., and Tamm, E.: Comparative study of nucleation mode aerosol particles and intermediate air ions formation events at three sites, *J. Geophys. Res.*, 109, D17201, doi:10.1029/2003JD004413, 2004.

Wang, M. and Penner, J. E.: Aerosol indirect forcing in a global model with particle nucleation, *Atmos. Chem. Phys.*, 9, 239–260, doi:10.5194/acp-9-239-2009, 2009.

Wiedensohler, A., Cheng, Y. F., Nowak, A., Wehner, B., Achtert, P., Berghof, M., Birmili, W., Wu, Z. J., Hu, M., Zhu, T., Takegawa, N., Kita, K., Kondo, Y., Lou, S. R., Hofzumahaus, A., Holland, F., Wahner, A., Gunthe, S. S., Rose, D., Su, H., and Pöschl, U.: Rapid aerosol particle growth and increase of cloud condensation nucleus activity by secondary aerosol formation and condensation: a case study for regional air pollution in northeastern China, *J. Geophys. Res.*, 114, D00G08, doi:10.1029/2008JD010884, 2009.

Wiedensohler, A., Birmili, W., Nowak, A., Sonntag, A., Weinhold, K., Merkel, M., Wehner, B., Tuch, T., Pfeifer, S., Fiebig, M., Fjåraa, A. M., Asmi, E., Sellegri, K., Depuy, R., Venzac, H., Villani, P., Laj, P., Aalto, P., Ogren, J. A., Swietlicki, E., Williams, P., Roldin, P., Quincey, P., Hüglin, C., Fierz-Schmidhauser, R., Gysel, M., Weingartner, E., Riccobono, F.,

ACPD

14, 9225–9247, 2014

## Source areas and trajectories of nucleating air masses

Z. Németh and I. Salma

Title Page

Abstract

Introduction

Conclusions

References

Tables

Figures

◀

▶

◀

▶

Back

Close

Full Screen / Esc

Printer-friendly Version

Interactive Discussion



**Source areas and trajectories of nucleating air masses**

Z. Németh and I. Salma

Title Page

Abstract

Introduction

Conclusions

References

Tables

Figures

◀

▶

◀

▶

Back

Close

Full Screen / Esc

Printer-friendly Version

Interactive Discussion

- Santos, S., Grüning, C., Faloon, K., Beddows, D., Harrison, R., Monahan, C., Jennings, S. G., O'Dowd, C. D., Marinoni, A., Horn, H.-G., Keck, L., Jiang, J., Scheckman, J., McMurry, P. H., Deng, Z., Zhao, C. S., Moerman, M., Henzing, B., de Leeuw, G., Löschau, G., and Basting, S.: Mobility particle size spectrometers: harmonization of technical standards and data structure to facilitate high quality long-term observations of atmospheric particle number size distributions, *Atmos. Meas. Tech.*, 5, 657–685, doi:10.5194/amt-5-657-2012, 2012.
- Young, L. H., Benson, D. R., Montanaro, W. M., Lee, S. H., Pan, L. L., Rogers, D. C., Jensen, J., Stith, J. L., Davis, C. A., Campos, T. L., Bowman, K. P., Cooper, W. A., and Lait, L. R.: Enhanced new particle formation observed in the northern midlatitude tropopause region, *J. Geophys. Res.*, 112, D10218, doi:10.1029/2006jd008109, 2007.
- Yu, F., Luo, G., Bates, T. S., Anderson, B., Clarke, A., Kapustin, V., Yantosca, R. M., Wang, Y., and Wu, S.: Spatial distributions of particle number concentrations in the global troposphere: simulations, observations, and implications for nucleation mechanisms, *J. Geophys. Res.*, 115, D17205, doi:10.1029/2009JD013473, 2010.



## Source areas and trajectories of nucleating air masses

Z. Németh and I. Salma

**Table 1.** Ranges, medians and means with standard deviations of the wind speed for all measurement days, and separately for non-nucleation days, for nucleation and growth intervals of class 1A events at the city centre and near-city background.

Site/statistics	All days	Non-nucleation days	Nucleation intervals
City centre			
minimum	0.10	0.10	0.15
median	2.6	2.4	2.7
maximum	15.8	15.8	13.2
mean	3.0	2.8	3.1
std. deviation	2.0	1.85	1.73
Near-city background			
minimum	< 0.10	< 0.10	< 0.10
median	< 0.10	< 0.10	0.30
maximum	3.1	2.7	3.1
mean	0.24	0.25	0.46
std. deviation	0.43	0.43	0.58

[Title Page](#)
[Abstract](#)
[Introduction](#)
[Conclusions](#)
[References](#)
[Tables](#)
[Figures](#)
[◀](#)
[▶](#)
[◀](#)
[▶](#)
[Back](#)
[Close](#)
[Full Screen / Esc](#)
[Printer-friendly Version](#)
[Interactive Discussion](#)

# Source areas and trajectories of nucleating air masses

Z. Németh and I. Salma

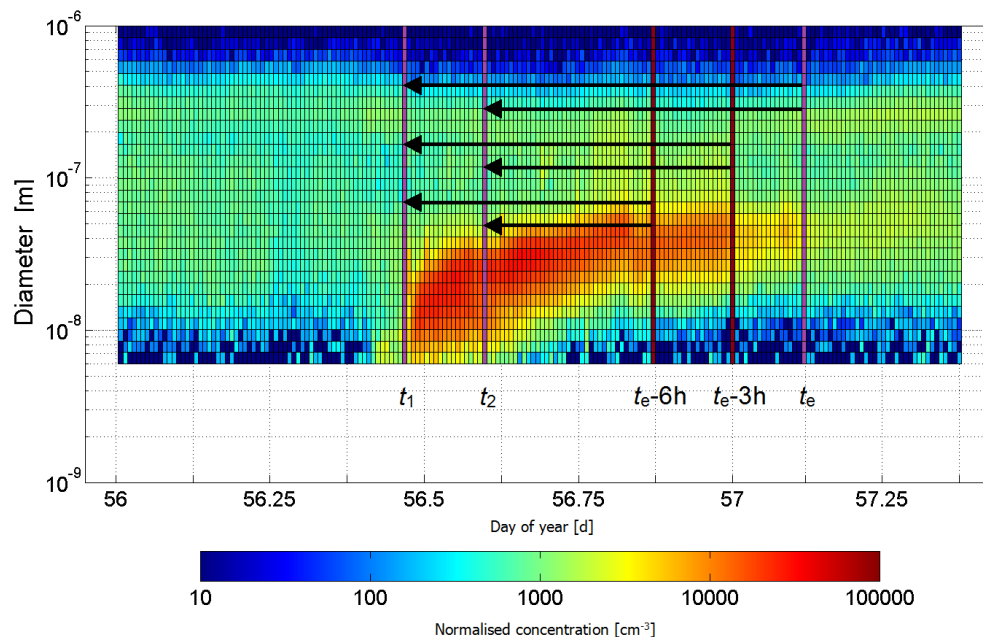


**Fig. 1.** Determination of the start ( $t_1$ ) and end ( $t_2$ ) time parameters of the nucleation, and the end of the particle growth ( $t_e$ ). The three arrow pairs correspond to three backward trajectories arriving to the measurement site at times of  $t_e$ ,  $t_e - 3$  h and  $t_e - 6$  h, and determine three limiting segmental pairs corresponding to  $t_e - t_1$ ,  $t_e - t_2$ , and  $t_e - 3$  h -  $t_1$ ,  $t_e - 3$  h -  $t_2$ , and  $t_e - 6$  h -  $t_1$ ,  $t_e - 6$  h -  $t_2$  on the air mass trajectories.

[Title Page](#)
[Abstract](#)
[Introduction](#)
[Conclusions](#)
[References](#)
[Tables](#)
[Figures](#)
[◀](#)
[▶](#)
[◀](#)
[▶](#)
[Back](#)
[Close](#)
[Full Screen / Esc](#)
[Printer-friendly Version](#)
[Interactive Discussion](#)

# Source areas and trajectories of nucleating air masses

Z. Németh and I. Salma

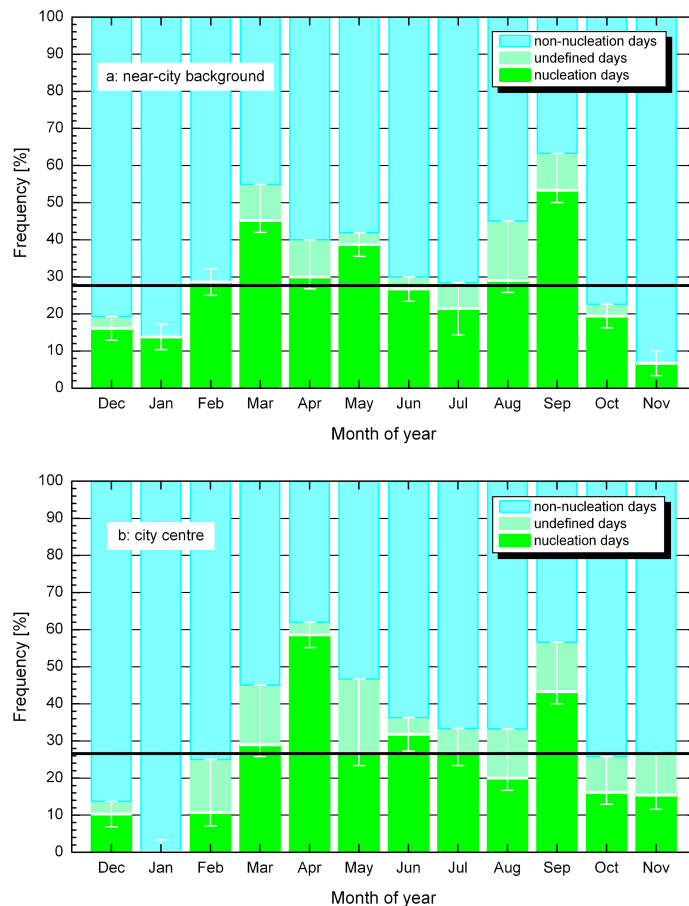


**Fig. 2.** Monthly mean frequencies for days with new particle formation, undefined days and non-event days in the near-city background (a) and city centre (b). The horizontal lines indicate yearly mean frequencies. For explanation of the error bars, see the text.

[Title Page](#)
[Abstract](#)
[Introduction](#)
[Conclusions](#)
[References](#)
[Tables](#)
[Figures](#)
[◀](#)
[▶](#)
[◀](#)
[▶](#)
[Back](#)
[Close](#)
[Full Screen / Esc](#)
[Printer-friendly Version](#)
[Interactive Discussion](#)

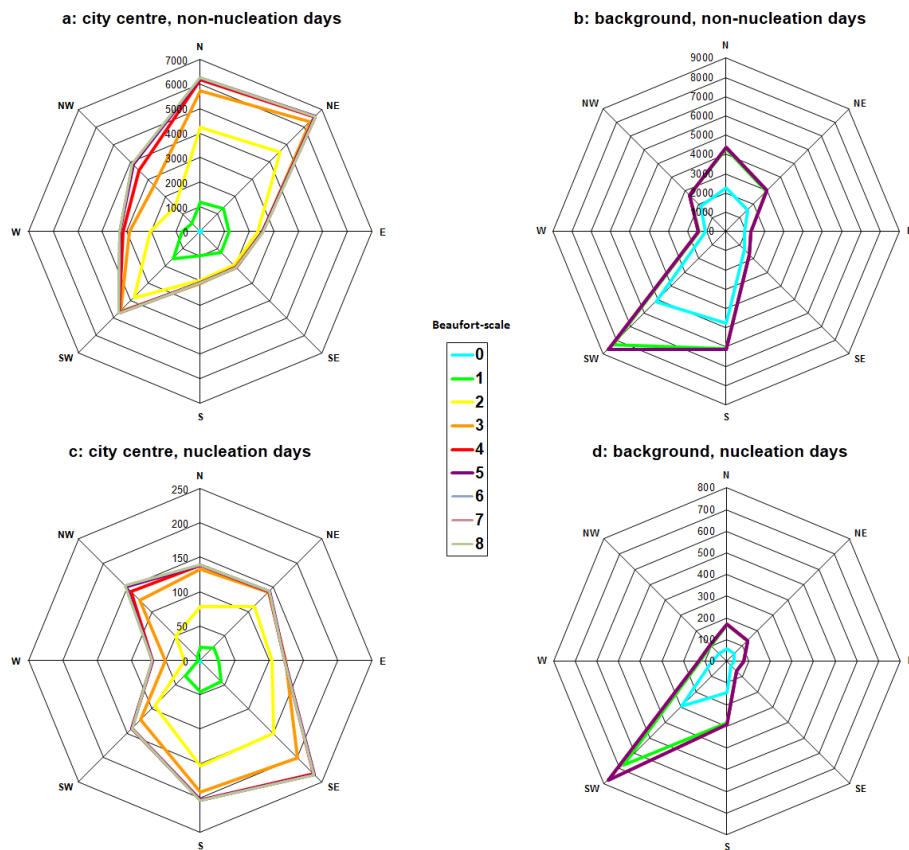


**Fig. 3.** Wind roses for non-nucleation days **(a)**, and for nucleation and growth intervals of class 1A events **(c)** in the city centre, and for non-nucleation days **(b)**, and for nucleation and growth intervals of class 1A events **(d)** in the near-city background.



**Fig. 4.** Tracks of nucleating air masses in and near the Carpathian Basin arriving to the city centre of Budapest. The overlapping track sections were indicated in stronger shaded colours (from yellow to orange).

## Source areas and trajectories of nucleating air masses

Z. Németh and I. Salma

Title Page

Abstract

Introduction

Conclusions

References

Tables

Figures

◀

▶

◀

▶

Back

Close

Full Screen / Esc

Printer-friendly Version

Interactive Discussion

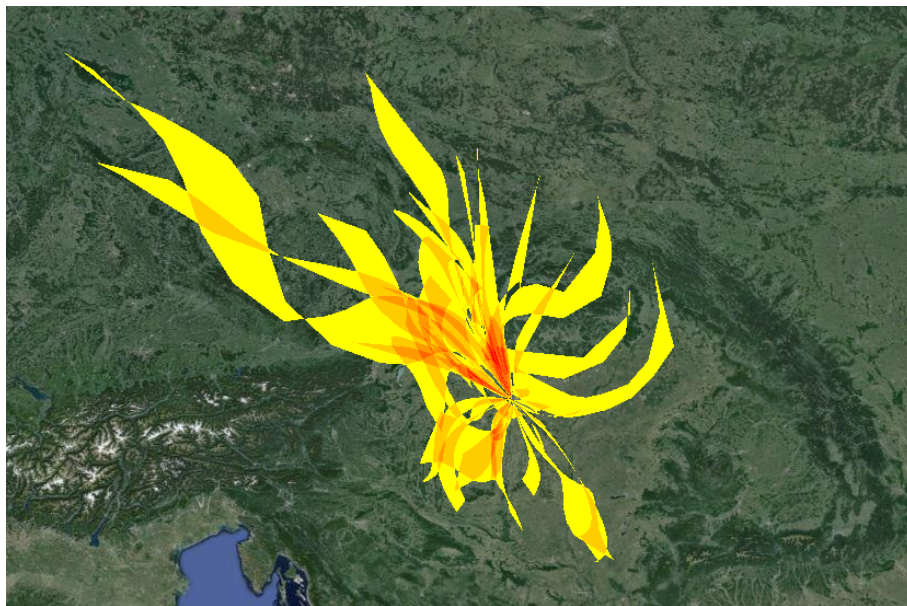


**Fig. 5.** Tracks of nucleating air masses in and near the Carpathian Basin arriving to the near-city background of Budapest. The overlapping track sections were indicated in stronger shaded colours (from yellow through orange to red).

## Source areas and trajectories of nucleating air masses

Z. Németh and I. Salma

Title Page

Abstract

Introduction

Conclusions

References

Tables

Figures

◀

▶

◀

▶

Back

Close

Full Screen / Esc

Printer-friendly Version

Interactive Discussion



## Source areas and trajectories of nucleating air masses

Z. Németh and I. Salma

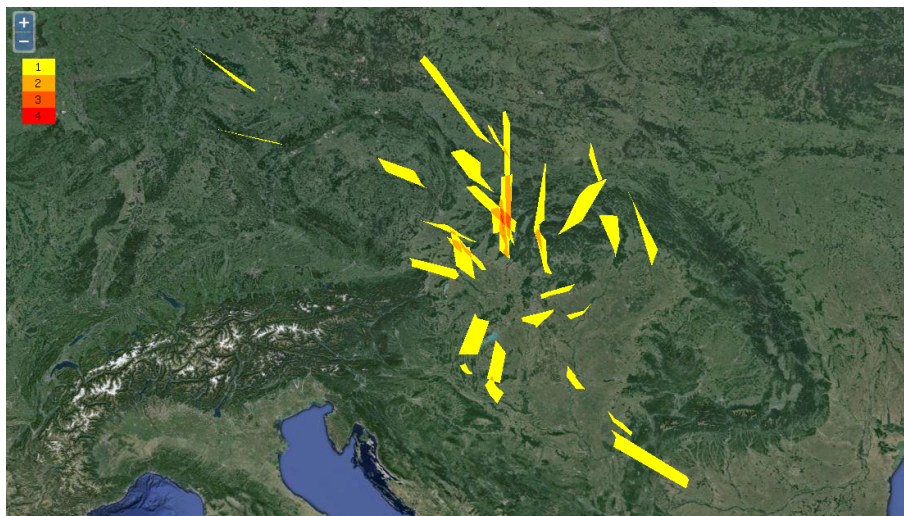


**Fig. 6.** Source regions of nucleating air masses within and near the Carpathian Basin arriving to the receptor site in Budapest (indicated by white dot). The overlapping source areas were indicated in stronger shaded colours (from yellow to red), and their multiplicity in overlapping is shown in the upper left corner.

[Title Page](#)[Abstract](#)[Introduction](#)[Conclusions](#)[References](#)[Tables](#)[Figures](#)[◀](#)[▶](#)[◀](#)[▶](#)[Back](#)[Close](#)[Full Screen / Esc](#)[Printer-friendly Version](#)[Interactive Discussion](#)